

Automated Features Extraction Of Optic Nerve

Miss Seema M. Labdi¹, Prof. J. P. Gawande²

¹M.E.II Year Bio- instrumentation, CCOE, Pune, India

²Bio- instrumentation, CCOE, Pune, India

ABSTRACT: *This project presents a novel automated method for fully automated detection of optic disk boundary in fundus images. The proposed method improves and extends the original snake (deforming-only technique) in two aspects: boundary detection of optic disk and center finding of cup. Morphological operator is used in this algorithm. The contour points are first self-separated into edge-point group or uncertain-point group by clustering after each deformation, and these contour points are then updated by different criteria based on different groups. The updating process combines both the local and global information of the contour to achieve the balance of contour stability and accuracy. The modifications make the proposed algorithm more accurate and robust to blood vessel occlusions, noises, ill-defined edges and fuzzy contour shapes. The comparative results show that the proposed method can estimate the disk boundaries of 30 test images closer to the groundtruth, with the better success rate when compared to doctors decision. In this project Matlab 7.1 is used.*

Keywords: *ASM, GVF, Matlab7.5, Morphological operator, glaucoma.*

I. INTRODUCTION

Glaucoma is a leading cause of blindness globally. In glaucoma, early progression of the disease often goes unnoticed by the individual due to the pattern of glaucomatous visual loss which proceeds inwards from the peripheral visual field view. As such, when visual loss is noticeable by the individual, severe progression of the disease has already occurred, with irrecoverable sight loss. This emphasizes the need for screening system for the early detection of glaucoma to allow timely intervention in order to save sight. However current glaucoma detection method is manual and impractical for screening.

Optic disk, fovea and blood vessels are the main component of the retina. Any change in the shape and colour of the optic disk is an indicator of various ophthalmic pathologies, essentially for glaucoma. Moreover, the optic disk boundary acts as a reference contour to measure other disk parameters, such as cup edges. In computer aided process of detection and screening of the diseases using colour fundus images, automated localization of the optic disk and estimation of its boundary are the first two essential steps before any further analysis.

An essential pathological characteristic in the progression of glaucoma is the increase in the size of the optic cup with respect to the optic disc. The optic disc, or optic nerve head, is the region in the retina where the optic nerve fibers, or ganglion cells, aggregate to form the optic nerve, which is connected to the brain. Within this optic disc is a depression known as the optic cup. During glaucomatous progression the death of the ganglion nerve cells leads to increased excavation of the optic cup and thus increases the CDR. Currently CDR evaluation is manually performed and is subject to individual evaluation by ophthalmologist. CDR is cup to disk ratio.

Currently, deformable models offer a reasonable approach for boundary detection and image segmentation which can be roughly classified in two categories: free-form deformable

models, such as snakes, and parametrically deformable models, such as active shape models (ASM). Dumitras and Venetsanopoulos compared four snake models (traditional, distance, balloon and gradient vector flow snake models) with respect to their accuracy in describing the shape of an object and robustness to changes of model parameter values. Their experimental results showed that both distance snake and gradient vector flow snake (GVF-snake) obtained more accurate results; and the GVF-snake outperformed other snakes in terms of robustness. Extracted the optic disk boundary by using the GVF-snake algorithm, in which the blood vessel was

first removed by gray-level morphology in the preprocessing step. Then, the disk boundary was initially located manually, and further refined through the GVF-snake algorithm. First, color morphology was employed to remove the blood vessels. Second, the authors used a template

matching to automatically initialize disk boundary. Although the morphology preprocessing helps reduce the effect of blood vessels, it could not totally remove the effect. Additionally, the

morphology preprocessing also blurs the optic disk boundary and changes its location, which could make the disk boundary detection unreliable. Presented a different template to locate the position of optic disk. The disk boundary was then segmented by a global deformation based on a global elliptic model and a local deformable model with variable edge-strength dependent stiffness. Their method was able to partly avoid occlusions of blood vessels. However, the authors indicated the performance to the images with variably pathological changes still needed to be further improved.

II. OPTIC DISK BOUNDARY DETECTION BY CENTROID METHOD

From the analysis of three colour channel the red channel of the RGB image is used here for computation because the blood vessel has relatively small effect and optic disk is sufficiently obvious in this channel. The candidate region of optic disk can be located with high probability by the largest bright region of the image $I(u,v)$, where u and v are the row and column numbers. The extraordinary case in which the pathological bright region is much larger and brighter than the optic disk is not considered in this paper, because it is a relatively rare case in the narrow-angle optic disk images. The median filter with relative large window is first applied on the original image to remove the effect of the pathological bright regions. From the observation, the average radius of the optic disk is approximately 55 pixels in our fundus image data. Hence the average disk region is close to 13% of the whole image area. For every filtered image, all pixels are listed in descending order of gray-level; the top 13% pixels are selected as the candidate region of the optic disk. The centroid of the selected pixels is set to be the initial disk center denoted as $c_0(u_0, v_0)$. Template matching could also be used to detect initial disk center. An error of the initial disk center within several dozen pixels could be tolerated because the initial center only provides the rough location of optic disk.[1]

2.1 Morphological Operator

Morphological operations are affecting the form, structure or shape of an object. Applied on binary images (black & white images – Images with only 2 colors: black and white) as shown in fig1. They are used in pre or post processing (filtering, thinning, and pruning) or for getting a representation or description of the shape of objects/regions (boundaries, skeletons convex hulls).[]

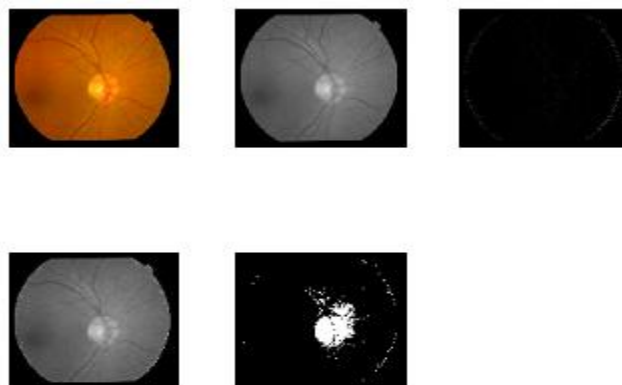


Fig1: comparisons of intensity in different channel of colour optic disk image

The two principal morphological operations are dilation and erosion. Dilation allows objects to expand, thus potentially filling in small holes and connecting disjoint objects. Erosion shrinks objects by etching away (eroding) their boundaries. These operations can be customized for an application by the proper selection of the structuring element, which determines exactly how the objects will be dilated or eroded.

The dilation process is performed by laying the structuring element B on the image A and sliding it across the image in a manner similar to convolution (will be presented in a next laboratory). The difference is in the operation performed. It is best described in a sequence of steps:

1. If the origin of the structuring element coincides with a 'white' pixel in the image, there is no change; move to the next pixel.
2. If the origin of the structuring element coincides with a 'black' in the image, make black all pixels from the image covered by the structuring element.

Notation:

$$AB \oplus$$

The structuring element can have any shape. Typical shapes are presented bellow

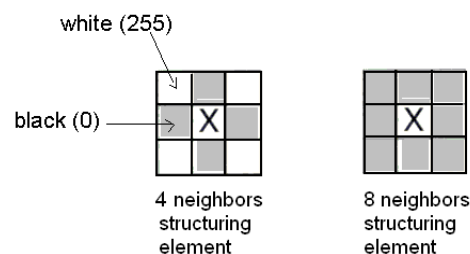


Fig. 2 Typical shapes of the structuring elements (B)

The *erosion* process is similar to dilation, but we turn pixels to 'white', not 'black'. As before, slide the structuring element across the image and then follow these steps:

1. If the origin of the structuring element coincides with a 'white' pixel in the image, there is no change; move to the next pixel.
2. If the origin of the structuring element coincides with a 'black' pixel in the image, and at least one of the 'black' pixels in the structuring element falls over a white pixel in the image, then change the 'black' pixel in the image (corresponding to the position on which the center of the structuring element falls) from 'black' to a 'white'.

Notation:

$$AB \ominus$$

In Fig. 7.4, the only remaining pixels are those that coincide to the origin of the structuring element where the entire structuring element was contained in the existing object. Because the structuring element is 3

pixels wide, the 2-pixel-wide right leg of the image object was eroded away, but the 3-pixel-wide left leg retained some of its center pixels

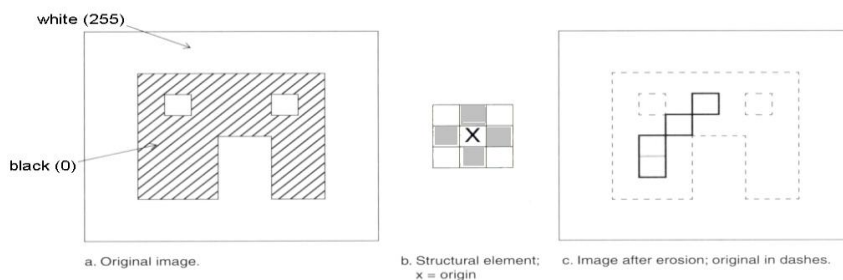


Fig. 3 Illustration of the erosion process

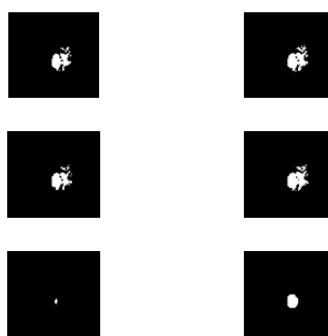


Fig4: Optic Disk after morphological operation.

III. MULTI-SCALE BLOOD VESSEL EXTRACTION

In our approach, color images input from the fundus camera are initially resized to a standard size of 768×576 pixels while maintaining the original aspect ratio. We select the green channel for all our operations because retinal images are almost always saturated in the red channel and have very low contrast in the blue channel. A closing operation is performed on the green channel image using two different sizes of a structuring element (filter). Closing operation is defined as dilation (Max filter) followed by erosion (Min filter). The formulations of dilation and erosion for gray scale images are as follows.

Dilation:

$$A \oplus B = A1(x, y) = \max_{i,j \in B} (A(x - i, y - j) + B(i, j))$$

Erosion:

$$A \ominus B = A2(x, y) = \min_{i,j \in B1} (A(x - i, y - j) + B1(i, j))$$

where A is the input image, B and B1 are the structuring elements or masks used for dilation and erosion respectively.

Dilation in gray scale enlarges brighter regions and closes small dark regions. The erosion is necessary to shrink the dilated objects back to their original size and shape. The dark regions closed by dilation do not respond to erosion. Thus, the vessels being thin dark segments laid out on a brighter background are lost by such a closing operation. A subtraction of the closed images across two different scales (let S1 and S2 be the sizes of the structuring elements B1 and B2) will thus give the blood vessel segments of the

green channel image. The operation is as follows

$$C' = (A \oplus B2) \ominus B2 - (A \oplus B1) \ominus B1$$

We use a disk shaped structuring element for morphological operations. The radius of the larger disk (S2) is fixed at a high value (we use 6 pixels for an image of size 768 × 576 pixels) so that all the vessels including the main blood vessel get closed. S1 is chosen adaptively as follows:

1. 1 or 2 pixels below S2 if we want to obtain only the thicker vessels emanating from the optic disk.
2. Atleast 4 pixels below S2 to obtain the entire blood vessel network.

Criterion 1 is used for optic disk localization whereas criterion 2 is used in microaneurysms and hemorrhages detection. The image C' is thresholded (90% of the maximum intensity) and median filtered to obtain the binary image of the blood vessels (U). Morphological thinning is then performed on U to obtain the skeleton of the blood vessel network. Thinning operation is implemented as

$U - (U \ominus B1 - U \ominus B2)$, where B1 and B2 are disjoint structuring elements and U is the complement of the image U. Noise can occur in the thinned image usually in the form of dots. A 2×2 median filtering operation is performed to remove the isolated specks of noise. The vessel segments being connected structures are unaffected by this operation. An additional source of noise in retinopathic images could be exudates. Fig4 shows the result of the vessel extraction algorithm on an image having no exudates.[3]

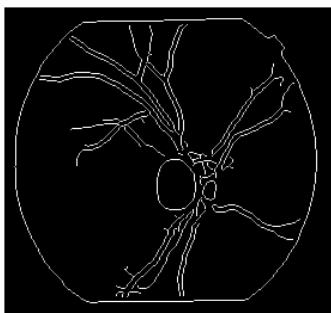


Fig:5 Illustration of the multi-scale vessel Extraction of optic disk image

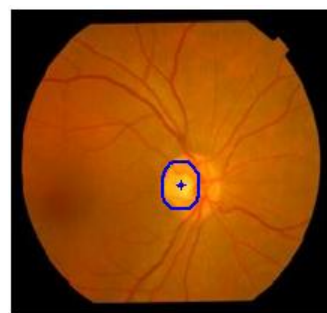


Fig6:Localization of cup centre and boundary

IV. ELLIPSE OPTIMIZATION FOR OPTIC DISK AND CUP

Ellipse fitting algorithm can be used to smooth the disc and cup boundary. Ellipse fitting is usually based on least square fitting algorithm which assumes that the best-fit curve of a given type is the curve that has the minimal sum of the deviations squared from a given data points[2] (least square error).

Direct Least Square Fitting Algorithm is chosen to fit the optic and cup over other popular ellipse fitting algorithms like Bookstein Algorithm and Taubin Algorithm. Instead of fitting general conics or being computationally expensive, this algorithm minimizes the algebraic distance subject to a constraint, and incorporates the ellipticity constraint into the normalization factor. It is ellipsespecific, thus the effect of noise (ocular blood vessel, hemorrhage, drusens, etc.) around the cup area can be minimized while forming the ellipse. It can also be easily solved naturally by a generalized Eigen system.

In Fitting algorithm, a quadratic constraint is set on the parameters to avoid trivial and unwanted solutions. The goal is to search a vector parameter which contains the six coefficients of the standard form of a conic.

An ellipse is a special case of a general conic which can be described by an implicit second order polynomial

$$F(x, y) = ax^2 + bxy + cy^2 + dx + ey + f = 0 \quad (1)$$

with an ellipse-specific constraint

$$b^2 - 4ac < 0 \quad (2)$$

Where a, b, c, d, e, f are coefficients of the ellipse and (x,y) are co- ordinates of points lying on it. The polynomial F(x, y) is called the algebraic distance of the point (x, y) to the given conic. By introducing vectors

$$\mathbf{a} = [a, b, c, d, e, f]^T$$

$$\mathbf{x} = [x^2, xy, y^2, x, y, 1] \quad (3)$$

it can be rewritten to the vector form

$$Fa(\mathbf{x}) = \mathbf{x} \cdot \mathbf{a} = 0 \quad (4)$$

The fitting of a general conic to a set of points (x_i, y_i) , $i = 1 \dots N$ may be approached by minimizing the sum of squared algebraic distances of the points to the conic which is represented by the coefficient \mathbf{a}

The problem (5) can be solved by the standard least squares approach, but the result of such fitting is a general conic and it need not to be an ellipse. To ensure an ellipse-specificity of the solution, the appropriate constraint (2) have to be considered. Under a proper scaling, the inequality constraint in (2) can be changed into an equality constraint.

$$4ac - b^2 = 1 \quad (6)$$

and the ellipse-specific fitting problem can be reformulated as

$$\min \|\mathbf{D}\mathbf{a}\|^2 \text{ subject to } \mathbf{a}^T \mathbf{C} \mathbf{a} = 1 \quad (7)$$

where the design matrix \mathbf{D} of the size $N \times 6$, represents the least squares minimization of (5) and the constraint matrix \mathbf{C} of the size 6×6 , express the constraint of (6). The minimization problem (7) is ready to be solved by a quadratically constrained least squares minimization.

First, by applying the Lagrange multipliers we get the following conditions for optimal solution \mathbf{a} .

$$\begin{aligned} \mathbf{S}\mathbf{a} &= -\mathbf{C}\mathbf{a} \\ \mathbf{a}^T \mathbf{C} \mathbf{a} &= 1 \end{aligned} \quad (8)$$

where \mathbf{S} is the scatter matrix of the size 6×6 ,

$$\mathbf{S} = \mathbf{D}^T \mathbf{D} \quad (9)$$

Next, Eq. (8) is solved by using generalized Eigen vectors. There exist up to six real solutions, but by considering the minimization $\|\mathbf{D}\mathbf{a}\|^2$ subjected to the constraint (6) would yield only one solution, which corresponds by virtue of constraint, to an ellipse.

Convex hull based Ellipse Optimization

A convex hull of a set of points is the smallest convex polygon that contains every one of the points. It is defined by a subset of all the points in the original set.

The convex hull of X can also be described constructively as the set of convex combinations of finite subsets of points from X : that is, the set of points of the form $\sum_{j=1}^n t_j x_j$, where n is an arbitrary natural number, the numbers t_j are nonnegative and sum to $\mathbf{1}$, and the point's x_j are in X .

If X is a subset of an N -dimensional vector space, convex combinations of at most $N+1$ points are sufficient in the definition above. This is equivalent to saying that the convex hull of X is the union of all simplexes with at most $N+1$ vertex.

Fig. 6 shows how convex hull was applied in our system in selecting feature points around the neuro-retina cup region. The pixel set obtained from level set method for cup region were usually segmented with the influence of the interweavement of surrounding ocular blood vessels, hemorrhages, drusens and other noises. If all those pixels were fed to ellipse fitting algorithm, they could yield an unreal cup boundary. Using feature points selected from the pixel set using convex hull to fit the ellipse cup the system could generate more realistic neuro-retinal cup.[3]

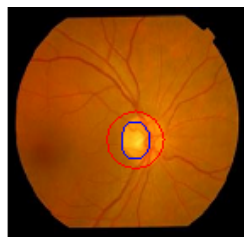


Fig7 ellipse fitted optic cup and disk

V. ROI DETERMINATION

In order to extract the optic disc and cup, a region of interest around the optic disc must first be delineated, as the optic disc generally occupies less than 5% of the pixels in a typical retinal fundus image.

While the disc and cup extraction can be performed on the entire image, localizing the ROI would help to reduce the computational cost as well as improve segmentation

accuracy. To localize the boundary exactly the component labeling method is used. In the images, regions are labelled by using the neighbourhood connecting pixels. All the connected pixels with the same input value are assigned the same identification label. The component labelling method The optic disc region is usually of a brighter pallor or higher color intensity than the surrounding retinal area.

This characteristic is exploited through automatically selecting 0.5% of the pixels in the image with the highest intensity. Next, the retinal image is subdivided into 64 regions, and an approximate ROI centre is selected based on the region containing the highest number of pre-selected pixels. Following this, the ROI is defined as a rectangle around the ROI centre with

dimensions of twice the typical optic disc diameter, and is used as the initial boundary for the optic disc segmentation, as shown in Figure 7.[4]

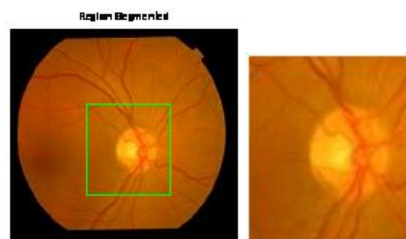


Fig 8: Region of interest segmentation

VI. CONCLUSION

A batch of 32 retinal fundus images from Dinanatha mangeshkar Hospital Pune, was obtained for processing. All colour fundus image data were first resize to 260X275 pixels. 32 images were randomly selected and tested, 25 images were successfully processed; 7 images required further improvement. Average computing time is 10 seconds.

TABLE1: Optic Disk Parameters After Image Processing

IMAGE	DIAMETER	AREA	PERCENTAGE	RESULT
FIG1	29.1856	669	0.49	NORMAL
FIG2	37.4581	1102	4.82	AB
FIG3	28.8565	654	0	NORMAL
FIG4	33.4731	880	2.6	AB
FIG5	54.4786	2331	17.11	AB
FIG9	79.3725	4948	43.28	AB
FIG11	28.3221	630	0.1	NORMAL
FIG12	84.2892	5580	49.6	AB
FIG13	36.19	1029	4.09	AB
FIG14	53.7966	2273	16.53	AB
FIG15	40.4646	1286	6.66	AB
FIG17	74.6438	4376	37.56	AB
FIG18	37.7796	1121	5.01	AB
FIG19	37.0995	1081	4.61	AB
FIG20	71.0431	3964	33.44	AB
FIG21	31.3113	770	1.5	AB
FIG22	28.7681	650	0	NORMAL
FIG23	48.5465	1851	12.31	AB
FIG24	57.7902	2623	20.03	AB

FIG25	48.244	1828	12.08	AB
FIG26	28.8565	654	0	NORMAL
FIG27	28.8565	654	0	NORMAL
FIG31	28.78	655	0	NORMAL
FIG32	54.4786	2331	17.11	AB

REFERENCES

Proceedings Papers:

- [1] Juan Xu, Opas Chutatape, and Paul Chew, Automated Optic Disk Boundary Detection by Modified Active Countour model, *roc. 2 IEEE Transaction on biomedical engineering Vol. 54, No. 3, March 2007*
- [2] A. Murthi, M Madheswaran, Enhancement of Optic cup to Disk Ratio Detection In Glaucoma diagnosis, *IEEE2012 International Conference on Computer Communication and Informatics (ICCCI-2012). Jan 10-12, 2012, Coimbatore, India*
- [3] Anonymous CCPR submission, *Automated feature Extraction for early Detection of Dianetic Retinopathy in Fundus Images, CVPR 2009 Submission*
- [4] J. Liu, D. W. K. Wong, J. H. Lim, X. Jia, F. Yin, H. Li, and W. Xiong, T. Y. Wong, Optic Cup nd Disk Extraction Fundus Image For Determination of Cup-to-Disk ratio. *IEEE 2008,*